International Journal of New Developments in Engineering and Society
ISSN 2522-3488 Vol. 8, Issue 4: 30-42, DOI: 10.25236/IJNDES.2024.080405

The hierarchical scheduling of the power system considering coordinated operation of source-load-storage sides

Jiaxuan Hu[1,*], Jianfeng Huang[2]

[1]*Electric Power College, Inner Mongolia University of Technology, Hohhot, 010080, China*
[2]*Electronics and Information Engineering, North China Institute of Science and Technology, Langfang, 065201, China*
[*]*Corresponding author*

Abstract: *The swift evolution of advanced power systems has resulted in a substantial rise in the share of renewable energy sources within these networks, which poses a challenge to the system's scheduling capabilities due to its inherent instability. In order to meet the demands for flexibility and to facilitate harmonious interaction among the diverse elements within the power system, this paper proposes an optimized configuration model for the power system based on the supply-demand relationship and coordinated operation among the power generators in source-load-storage sides. The model combines the operation flexibility of power supply and storage, as well as the overall flexibility. Constraints are imposed on the supply-demand relationship between the energy supply and load sides, and the output power of source sides and storage stations on the power supply and storage sides. An evaluation of the overall flexibility is conducted. This advanced scheduling model is designed to optimize by reducing the overall operational cost, achieving this goal through the definition of a specific objective function.. To address the nonlinear components in cost calculations, a quadratic function is segmented and linearized, and the CPLEX solver in MATLAB 2022a is utilized to obtain the optimal solution. Through case studies with three distinct scenarios, the viability and efficacy of the proposed model have been substantiated, demonstrating improved renewable energy consumption, reduced wind power curtailment, and made the load curve more stable.*

Keywords: *Renewable Energy Integration, Hierarchical Scheduling, Source-Storage-Load Coordinated Operation, Demand Response*

1. Introduction

Today, nne of the paramount issues that humanity is currently grappling with is global warming, with significant impacts on both human society and the natural environment. Under these circumstances, environmental protection and sustainable development have become the global consensus. Numerous works have indicated that the power system is a major gas emissions contributor leading to global greenhouse [1-2]. Consequently, a critical focus in recent studies has been the development of optimized scheduling strategies for power systems, aiming to curb carbon emissions and combat climate change through more efficient and sustainable energy management [3-4].

With the continuous advancement of renewable energy technologies and their expanding application domains, the novel power system has become a research hotspot [5]. Originating from the coordinated operation of source-load-storage sides and optimization model, the power system emphasizes the utilization of renewable energy sources such as solar, wind, and hydro to address environmental pollution, high renewable energy consumption, and unstable energy supply in traditional power systems. When it comes to power generation, renewable energy sources have taken the lead as the dominant contributor to new additions in power generation capacity. [6-7]. Additionally, remarkable progress has been made in power system construction and energy storage technologies [8-9]. However, with these advancements, the power system still faces challenges such as uncertainty and high coupling, which render traditional theoretical methodologies inadequate for addressing these complexities. The instability of the energy supply, stemming from the aging of energy production facilities and the restructuring of the power system, further compounds these challenges.

To address these issues, through the development of new operational approaches for power systems,

ISSN 2522-3488 Vol. 8, Issue 4: 30-42, DOI: 10.25236/IJNDES.2024.080405

studies have been carried out by researchers to boost the efficiency and stability of energy production facilities, ensuring a dependable energy supply. [10-11]. The utilization of renewable energy technologies has also been explored to reduce reliance on traditional energy sources and mitigate environmental pollution and energy consumption [12-13]. Although diverse renewable energy technologies, including those integral to new power system paradigms, can significantly enhance the utilization of novel energy sources, they continue to encounter hurdles in real-world implementation. For instance, diminishing the reliance on conventional fossil fuels, elevating the share of renewable energy in use, and securing the synchronized functioning of generation, consumption, and storage remain pressing challenges.

Based on the current research and various requirements of the power system, this paper adopts a scheduling optimization approach, which coordinates the source, load, and storage components. It considers the flexibility and stability of the electricity provision, energy storage, and load sides. the running flexibility of each generator and energy storage unit is analyzed. According to the flexibility constraints of generators and energy storage units and the demand response of the load side, an optimized scheduling model for the power system is established to reduce the total operation cost, which explores the optimal renewable energy consumption effect and cost reduction under different scenarios. Eventually, the feasibility and effectiveness of the validity of the proposed method is confirmed across various scenarios.

2. Establishment of the Source-Load-Storage Basic Model for Multi-Energy Power Systems

2.1 Operation Flexibility Constraints of the power system

The energy supply must adapt to the fluctuating demand from the load side, which can both increase and decrease of the energy power of the unit. This means load demand is constrained by both a maximum and a minimum power. Consequently, the operation flexibility must encompass both a maximum and a minimum flexibility to meet the system's energy demand. The following constraints are expressed by (1).

$$\begin{cases} F_{es,t}^{up} \geq F_{ls,t}^{up} \\ F_{es,t}^{un} \geq F_{ls,t}^{un} \end{cases} \tag{1}$$

where $F_{es,t}^{up}$ and $F_{es,t}^{un}$ are the maximum and minimum flexibility of energy supply over different time t,$F_{ls,t}^{up}$ and $F_{ls,t}^{un}$ respectively are the maximum and minimum of energy demand flexibility for the entire system at the time t.

The flexibility of energy demand corresponds to the load variation on the load side, and the $F_{es,t}^{up}$ and $F_{es,t}^{un}$ respectively are the maximum bounds of demand flexibility are expressed by (2).

$$\begin{cases} F_{ls,t}^{up} = max\left\{P_{ls,t+1}^{load,max} - P_{ls,t}^{load}, 0\right\} \\ F_{ls,t}^{un} = max\left\{P_{ls,t}^{load} - P_{ls,t+1}^{load,min}, 0\right\} \end{cases} \tag{2}$$

where $P_{ls,t}^{load}$ is the power on the load side at the time t, $P_{ls,t+1}^{load,max}$ and $P_{ls,t+1}^{load,min}$ respectively are the maximum and minimum of power fluctuations on the load-side at the subsequent time t+1.

2.2 Flexibility Constraints of Supply Resource and Energy Storage

The main resources for supplying energy to loads in this article include the flexibility provided by adjustable heating power generators, the flexibility considering hydroelectric generators, the flexibility offered by wind power generators, and the flexibility provided by pumped-storage hydropower plants through energy storage and release. Therefore, the flexibility offered by the power system can be expressed by (3).

$$\begin{cases} F_{es,t}^{up} = F_{tp,m,t}^{up} + F_{we,n,t}^{up} + F_{ps,u,t}^{up} + F_{wp,s,t}^{up} \\ F_{es,t}^{un} = F_{tp,m,t}^{un} + F_{we,n,t}^{un} + F_{ps,u,t}^{un} + F_{wp,s,t}^{un} \end{cases} \tag{3}$$

where $F_{tp,m,t}^{up}$,$F_{we,n,t}^{up}$,$F_{ps,u,t}^{up}$,$F_{wp,s,t}^{up}$ and $F_{tp,m,t}^{un}$, $F_{we,n,t}^{un}$,$F_{ps,u,t}^{un}$,$F_{wp,s,t}^{un}$ are the maximum and minimum flexibility provided by the adjustable thermal power system unit m, hydroelectric system unit n, pumped-storage hydropower system u, and wind power system unit s, respectively, for the power

ISSN 2522-3488 Vol. 8, Issue 4: 30-42, DOI: 10.25236/IJNDES.2024.080405

system at the time t.

The maximum and minimum flexibility provided by the adjustable thermal power system units can be expressed by (4).

$$\begin{cases} F_{tp,m,t}^{up} = min\{P_{tp,m}^{max} y_{tp,m,t} - P_{tp,m,t}, R_a^{up} y_{tp,m,t} \Delta t\} \\ F_{tp,m,t}^{un} = min\{P_{tp,m,t} - P_{tp,m}^{min} y_{tp,m,t}, R_a^{un} y_{tp,m,t} \Delta t\} \end{cases} \tag{4}$$

where $P_{tp,m,t}$ is the generation output from thermal power station m at time t, and $P_{tp,m}^{max}$ and $P_{tp,m}^{min}$ represent the upper and lower bounds for the output of active power unit m, R_a^{up} and R_a^{un} respectively represent the upper and lower ramp rates of the unit m, $y_{tp,m,t}$ denotes a 0 or 1 state indicator variable denoting the operation or shutdown status of the unit at the time t, Δt denotes the scheduling interval.

The flexibility of hydroelectric units in terms of ramping up and down can be expressed by (5).

$$\begin{cases} F_{we,n,t}^{up} = min\{P_{we,n}^{max} - P_{we,n,t}, R_b^{up} \Delta t\} \\ F_{we,n,t}^{un} = min\{P_{we,n,t} - P_{we,n}^{min}, R_b^{un} \Delta t\} \end{cases} \tag{5}$$

where $P_{we,n,t}$ is the output of hydroelectric unit n at the time t, $P_{we,n}^{max}$ and $P_{we,n}^{min}$ are the upper and lower bounds of the unit's active power output, R_b^{up} and R_b^{un} indicate the upper and lower ramp rates of hydroelectric unit n, Δt represents the scheduling interval.

The maximum and minimum flexibility provided by wind turbines to the system can be expressed by (6).

$$\begin{cases} F_{wp,s,t}^{up} = min\{P_{wp,n}^{max} - P_{wp,s,t}, R_c^{up} \Delta t\} \\ F_{wp,s,t}^{un} = min\{P_{wp,s,t} - P_{wp,n}^{min}, R_c^{un} \Delta t\} \end{cases} \tag{6}$$

where $P_{wp,s,t}$ is the output of wind turbine s at time t, $P_{wp,n}^{max}$ and $P_{wp,n}^{min}$ are the upper and lower bounds for the unit's output of active power, R_c^{up} and R_c^{un} are the ascending and descending ramp rates of wind energy converter s, Δt denotes the scheduling time interval.

The flexibility provided power via pumped-storage hydroelectric facilities for the system through energy storage and discharge can be expressed by (7).

$$\begin{cases} F_{ps,u,t}^{up} = min\left\{ \begin{matrix} P_{ps,u}^{G,max} - P_{ps,u,t}, \\ [(E_{ps,u,t} - E_{ps,u}^{min})/\eta_u^G - P_{ps,u,t}\Delta t]/\Delta t \end{matrix} \right\} \\ F_{ps,u,t}^{un} = min\left\{ \begin{matrix} P_{ps,u}^{P,max} + P_{ps,u,t}, \\ [(E_{ps,u}^{max} - E_{ps,u,t})/\eta_u^P - P_{ps,u,t}\Delta t]/\Delta t \end{matrix} \right\} \end{cases} \tag{7}$$

where $P_{ps,u,t}$ is the output of the pumped energy storage facility at time t, $P_{ps,u}^{G,max}$ and $P_{ps,u}^{P,max}$ are the maximum generation and pumping powers, respectively, $E_{ps,u,t}$,$E_{ps,u}^{max}$ and $E_{ps,u}^{min}$ are the upper reservoir capacity and its maximum and minimum limits for the hydroelectric pumped storage station at different time periods, η_u^G and η_u^P are the water loss coefficients for the hydroelectric pumped storage station u during power generation and pumping, respectively, Δt denotes the scheduling time interval.

In summary, the maximum and minimum flexibility supply of the system can be expressed by (8).

$$\begin{cases} F_t^{up} = \sum_{m=1}^{N_{tp}} F_{tp,m,t}^{up} + \sum_{n=1}^{N_{we}} F_{we,n,t}^{up} + \sum_{u=1}^{N_{ps}} F_{ps,u,t}^{up} + \sum_{s=1}^{N_{wp}} F_{wp,s,t}^{up} \\ F_t^{un} = \sum_{m=1}^{N_{tp}} F_{tp,m,t}^{un} + \sum_{n=1}^{N_{we}} F_{we,n,t}^{un} + \sum_{u=1}^{N_{ps}} F_{ps,u,t}^{un} + \sum_{s=1}^{N_{wp}} F_{wp,s,t}^{un} \end{cases} \tag{8}$$

where F_t^{up} and F_t^{un} are the maximum and minimum flexibility supply of the system energy measurement in the respective time periods, N_{tp}, N_{we}, N_{wp} and N_{ps} are the numbers of heating power plants, hydroelectric generators, wind energy turbines and pumped-storage hydro facilities, respectively.

ISSN 2522-3488 Vol. 8, Issue 4: 30-42, DOI: 10.25236/IJNDES.2024.080405

2.3 Modeling of Flexibility Demand

The errors in multi-energy power systems primarily stem from the indeterminacy associated with renewable energy generation, the volatility of load demand, and the prediction errors of load. The errors that arise during operation represent the flexibility demand of the power system's power sources. Similar to the aforementioned resource flexibility models, the flexibility demand model also has its maximum and minimum limits, which are divided into the system's maximum flexibility demand and minimum flexibility demand.

$$\begin{cases} \Delta Q_l = Q_{l,t+1} - Q_{l,t} \\ F_{p,t}^{up} = w_{up} Q_{w,t+1} + e_{up} Q_{l,t+1} + \Delta Q_l \\ F_{p,t}^{un} = w_{un} Q_w^{max} - Q_{w,t+1} + e_{un} Q_l^{max} - Q_{l,t+1} + \Delta Q_l \end{cases} \tag{9}$$

where $Q_{l,t+1}$ and $Q_{w,t+1}$ are the forecasted values of wind power and load power for the time t+1, $Q_{l,t}$ is the forecasted values of load power for the period t, ΔQ_l is the difference between the predicted values of load power for the time (t+1) and time t, $F_{p,t}^{up}$ and $F_{p,t}^{un}$ are the maximum and minimum flexibility demands of the system for the time t, w_{up}, w_{un} are the upper and lower bounds of flexibility coefficients caused by wind power prediction errors, e_{up}, e_{un} are the maximum and minimum flexibility coefficients caused by load power prediction errors, and Q_w^{max} and Q_l^{max} are the maximum values of wind power and load power, respectively.

2.4 System-wide Flexibility Evaluation

The overall flexibility margin assessment of the source-load-storage system is represented by the difference between the system's upper and lower bounds of flexibility supply and the power source's upper and lower bounds of flexibility demand. It is divided into system's maximum flexibility margin and minimum flexibility margin:

$$\begin{cases} \Delta F_t^{up} = F_t^{up} - F_{p,t}^{up} \\ \Delta F_t^{un} = F_t^{un} - F_{p,t}^{un} \end{cases} \tag{10}$$

where, ΔF_t^{up} and ΔF_t^{un} are the maximum flexibility margin and minimum flexibility margin of the system in the time t, respectively.

3. A Hierarchical Optimization Scheduling Model Considering Source-Load-Storage Integration

This paper studies the flexibility of power systems from three aspects. The energy supply system on the power supply side consists of three parts: thermal power generation units, hydroelectric generation units, and wind power generation units. The energy storage side utilizes pumped-storage power stations for electricity storage. In this paper, the energy supply side and the power storage aspect are combined into an integrated system to supply power to the load side, where the source-storage system of the power system provides and dispatches energy flexibility stemming from the demand-reactive mechanism of the load side.

3.1 Objective function

The principal focus of this paper is to explore the optimization of the source-storage subsystem within a multi-energy, source-load-storage power system framework, with particular emphasis on the load side's demand response dynamics. A hierarchical scheduling optimization model is established for the source-storage system, with the total operating cost as the optimization objective. Based on the flexibility supply, flexibility demand, and flexibility margin provided by the aforementioned model, optimization analyses are conducted from indicators such as unit cost and energy storage cost. The optimization scheduling model aims to minimize the total operating cost, designated as f_Σ, which comprises: the startup, shutdown, and operation cost of thermal power units (primarily fuel consumption cost) f_{tp}, the startup and shutdown cost of hydropower units f_{we}, the startup and shutdown cost of wind power units f_{wp}, the cost of pumped-storage power stations f_{ps}, and the penalty cost for wind curtailment and load shedding f_{pu}. Specifically:

$$f_\Sigma = \min\left(f_{tp} + f_{we} + f_{wp} + f_{ps} + f_{pu}\right) \tag{11}$$

ISSN 2522-3488 Vol. 8, Issue 4: 30-42, DOI: 10.25236/IJNDES.2024.080405

The startup, stop, and operation cost (primarily fuel consumption cost) of thermal power units f_{tp} can be expressed by (12).

$$f_{tp} = \sum_{t=1}^{T}\sum_{m=1}^{N_{tp}}(a_m P_{tp,m,t}^2 + b_m P_{tp,m,t} + c_m)y_{tp,m,t} + \sum_{t=1}^{T}\sum_{m=1}^{N_{tp}}[q_{tp,m,t}(1-q_{tp,m,t-1})f_{tp,m}^D + q_{tp,m,t-1}(1-q_{tp,m,t})f_{tp,m}^H] \tag{12}$$

where T is the total scheduling time, N_{tp} is the number of heating power units, a_m, b_m and c_m denote the coefficients of coal consumption of thermal power units, $q_{tp,m,t}$ is the start-stop variable of thermal power unit m, where $q_{tp,m,t}$=0 signals that the unit is in the non-operational state at time t, and $q_{tp,m,t}$=1 indicates that the unit is in the initiation state at time t ($q_{tp,m,t-1}$ and $q_{tp,m,t}$ have opposite states, indicating a transition from one state to another), $f_{tp,m}^D$ and $f_{tp,m}^H$ are the initiation expenses and cessation expenses of unit m.

The start-stop cost of hydropower units, denoted as f_{we}, can be expressed by (13).

$$f_{we} = \sum_{t=1}^{T}\sum_{n=1}^{N_{we}}[q_{we,n,t}(1-q_{we,n,t-1})f_{we,n}^D + q_{we,n,t-1}(1-q_{we,n,t})f_{we,n}^H], \tag{13}$$

where N_{we} is the number of hydropower units, $q_{we,n,t}$ is the start-stop variable of hydropower unit n, where $q_{we,n,t}$=0 indicates the unit is in stop state, and $q_{we,n,t}$=1 indicates the unit is in startup state ($q_{we,n,t-1}$ and $q_{we,n,t}$ have opposite states, indicating a transition from one state to another), $f_{we,n}^D$ and $f_{we,n}^H$ are the initiation expenses and cessation expenses of unit n.

The initiation - cessation cost of wind energy units,f_{wp} can be expressed by (14).

$$f_{wp} = \sum_{t=1}^{T}\sum_{u=1}^{N_{wp}}[q_{wp,u,t}(1-q_{wp,u,t-1})f_{wp,u}^D + q_{wp,u,t-1}(1-q_{wp,u,t})f_{wp,u}^H], \tag{14}$$

where N_{wp} is the number of wind power units, $q_{wp,u,t}$ is the start-stop variable of wind power unit u, where $q_{wp,u,t}$=0 indicates unit u is in the non-operational state at time t, and $q_{wp,u,t}$=1 indicates unit u is in the initiation state at time t ($q_{wp,u,t-1}$ and $q_{wp,u,t}$ have opposite states, indicating a transition from one state to another), $f_{wp,u}^D$ and $f_{wp,u}^H$ are the startup and stop costs of unit u.

With regard to pumped-storage hydroelectric facilities, the cost f_{ps} includes the startup-shutdown cost and energy storage operation cost, which can be expressed by (15).

$$f_{ps} = \sum_{t=1}^{T}\sum_{s=1}^{N_{ps}}[q_{ps,s,t}(1-q_{ps,s,t-1})f_{ps,s}^D + q_{ps,s,t-1}(1-q_{ps,s,t})f_{ps,s}^H] + \sum_{t=1}^{T}\sum_{j=1}^{N_B}C_j^B(P_{j,t}^D + P_{j,t}^H) \tag{15}$$

where N_{ps} and N_B are the number of pumped-storage hydroelectric facilities and batteries, respectively, $q_{ps,s,t}$ is the startup-stop status of pumped-storage hydroelectric facilities, where $q_{ps,s,t}$=0 indicates the station is in shutdown state at time t, and $q_{ps,s,t}$=1 indicates the station is in the initiation state at time t ($q_{ps,s,t-1}$ and $q_{ps,s,t}$ have opposite states, indicating a transition from one state to another), $f_{ps,s}^D, f_{ps,s}^H$ is the startup and stop costs of the power station. C_j^B is the expense coefficient per unit of charging and discharging for battery j, $P_{j,t}^D, P_{j,t}^H$ is the charging and discharging power of battery j at time t.

The penalty cost f_{pu} includes wind power curtailment cost and load shedding cost, it is expressed by (16).

ISSN 2522-3488 Vol. 8, Issue 4: 30-42, DOI: 10.25236/IJNDES.2024.080405

$$f_{pu} = \sum_{t=1}^{T}\sum_{u=1}^{N_{wp}} K_{wp}\Delta P_{wp,u,t}\Delta t + \sum_{t=1}^{T}\sum_{v=1}^{N_{ln}} K_{ln}\Delta P_{ln,v,t}\Delta t \tag{16}$$

where N_{wp}, N_{ln} are the number of wind power units and load nodes, K_{wp}, K_{ln} are the sanction cost per unit of wind energy curtailment and per unit of the load shedding, $\Delta P_{wp,u,t}, \Delta P_{ln,v,t}$ are the reduction of wind power output and the decrease in power supplied to the load, respectively.

3.2 Constraints of the proposed model

(1) Power balance constraint

$$\sum_{m=1}^{N_{tp}} P_{tp,m,t} + \sum_{n=1}^{N_{we}} P_{we,n,t} + \sum_{u=1}^{N_{wp}} P_{wp,u,t} + \sum_{s=1}^{N_{ps}} P_{ps,s,t} = Q_{l,t} - \sum_{v=1}^{N_{ln}} \Delta P_{ln,v,t} \tag{17}$$

(2) Hierarchical Scheduling Constraints of Source-Storage sides

As we delve into optimizing the scheduling of the source-storage side, taking into account the load side's demand response, the source-storage side can be divided into multiple scheduling layers, with respective constraints imposed. The detailed layers along with their respective restrictions are outlined as follows:

1) Heating Power Scheduling Layer

Considering the output power of thermal power units, the following constraints are imposed in this scheduling layer: the production bounds for heating power units and the unit's change-rate restrictions. These constraints can be expressed by (18) and (19).

$$P_{tp,m}^{min} \le P_{tp,m} \le P_{tp,m}^{max} \tag{18}$$

$$\begin{cases} P_{tp,t} - P_{tp,t-1} \le R_a^{up}\Delta t \\ P_{tp,t-1} - P_{tp,t} \le R_a^{un}\Delta t \end{cases} \tag{19}$$

where Eq. (18) is the output constraints of thermal power units, and Eq. (19) is the ramping constraints. In these equations, m represents the heat-generating power unit, t and $t-1$ represent the time periods, and 1 and 2 represent the electricity generation of the heating power unit m at time t and $t-1$, respectively.

2) Hydropower Scheduling Layer

The output constraints of hydropower units are imposed, which can be expressed as:

$$P_{we,n}^{min} \le P_{we,n,t} \le P_{we,n}^{max} \tag{20}$$

where Eq. (20) is the output constraints of hydropower units.

3) Wind Power Scheduling Layer

In wind power scheduling, the main consideration is the output constraints of wind energy generators, which can be expressed as:

$$P_{wp,u}^{min} \le P_{wp,u,t} \le P_{wp,u}^{max} \tag{21}$$

where Eq. (21) is the output bounds of wind power generators.

4) Energy Storage Scheduling Layer

In the scheduling of the energy storage components, the limitations on water reservoir capacity in reservoirs and the power input/output during the charging/discharging processes of the energy storage system are considered, which can be expressed by (22) and (23).

$$S_{ps}^{min} \le S_{ps} \le S_{ps}^{max} \tag{22}$$

ISSN 2522-3488 Vol. 8, Issue 4: 30-42, DOI: 10.25236/IJNDES.2024.080405

$$\begin{cases} P^{D,min} \le \sum_{t=1}^{T}\sum_{j=1}^{N_B} P_{j,t}^{D} \le P^{D,max} \\ P^{H,min} \le \sum_{t=1}^{T}\sum_{j=1}^{N_B} P_{j,t}^{H} \le P^{H,max} \end{cases} \tag{23}$$

where Eq. (22) represents the water storage constraints in reservoirs, where S_{ps} represents the water volume in the reservoir, and S_{ps}^{min} and S_{ps}^{max} represent the maximum and minimum limits of the reservoir storage volume. Eq. (23) represents the charging/discharging power constraints of energy storage, where $P^{D,min}$ and $P^{D,max}$ denote the maximum and minimum thresholds for the charging power, and $P^{H,min}$ and $P^{H,max}$ signify the maximum and minimum boundaries for the discharging power.

5) Other Operation Constraints

These encompasses limitations on wind power curtailment, conditions for load shedding, and stipulations regarding system flexibility. The constraints regarding wind power curtailment and load shedding can be delineated by equations (24) and (25).

$$0 \le \Delta P_{wp,u,t} \le P_{wp,u,t} \tag{24}$$

$$0 \le \Delta P_{ln,v,t} \le P_{ln,v,t} \tag{25}$$

where $P_{wp,u,t}$ and $P_{ln,v,t}$ are the reduction of wind power output and the decrease in load demand, respectively.

The operational flexibility constraints are represented by Eq. (1) to Eq. (9), and their evaluation metric is Eq. (10).

(3) The Method of Model Solution

To effectively solve the model, it becomes imperative to linearize both the model and its associated constraint conditions. Since the start-stop costs of heating power units are quadratic functions, they require piecewise linearization.

After the linearization process, the model and its constraint conditions are transformed into a linear programming model with mixed variables. The resolution of this model is accomplished utilizing the CPLEX solver, integrated within the MATLAB 2022a environment.

4. Scenario analysis

4.1 Scenario Introduction

To additionally evaluate the viability and efficacy of the proposed power system scheduling optimization in this paper, different scenarios based on the source-load-storage hierarchical scheduling are proposed to validate the computational scenario, Parameters are installed by various units and loads in this paper are as follows: the aggregate rated capacity of heating power units is 3796MW, the aggregate rated capacity of wind power units is 2000MW, the aggregate rated capacity of hydropower units is 2000MW, and the capability of the pumped-storage hydroelectric facility is 600MW. The power forecast curves for wind-generated electricity, hydropower, and load requirements are presented in Figure 1. The characteristic parameters and operation costs of units in the system are in accordance with the Table 1, Table 2 and Table 3.

Table 1: Heating power units' parameters

number	P_{max}/MW	a_m	b_m	c_m
1	646	4.8×10^{-4}	10.5	1675
2	725	5.2×10^{-4}	10.5	1139
3	652	4.8×10^{-4}	10.5	1675
4	508	5.6×10^{-4}	10.5	1500
5	687	6.0×10^{-4}	10.5	1675
6	580	5.6×10^{-4}	10.5	1500

ISSN 2522-3488 Vol. 8, Issue 4: 30-42, DOI: 10.25236/IJNDES.2024.080405

Table 2: Winging power units' parameters

Installed capacity(MW)	Running cost($/MW)	Abandoned wind cost($/MW)
2000	50	300

Table 3: Hydropower units' parameters

Installed capacity(MW)	Running cost($/MW)
2000	21

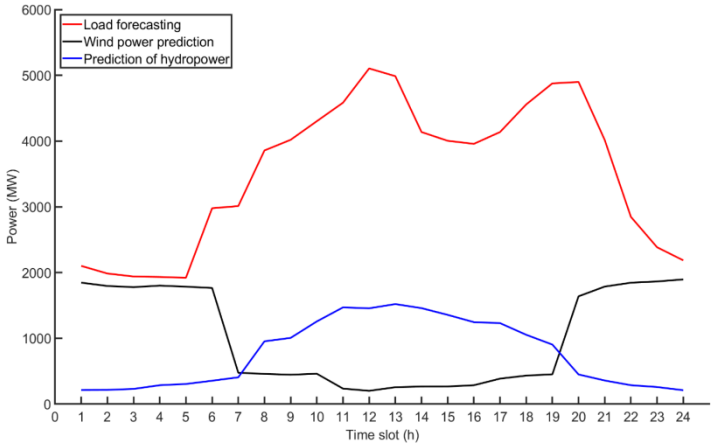

Figure 1: Wind Energy Generation and Demand Load Forecast Curves

In accordance with the established model and constraint conditions in this paper, three scenarios can be used to analyze the efficacy of the optimized scheduling scenario, specifically as follows:

Scenario 1: Without considering hierarchical scheduling, only the generation from the source side and the power consumption from the load side are considered.

Scenario 2: Hierarchical scheduling and coordinated operation of source and storage are considered, while the responsiveness of the load side to demand fluctuations are not considered.

Scenario 3: Considering hierarchical scheduling and the coordinated operation of the source-load-storage, where the flexibility of the load participates for load leveling and peak reduction.

4.2 Analysis of calculation results

(1) Analysis of Scenario 1

Figure 2 shows the generation output of units and the load curve under the coordinated operation of source and load.

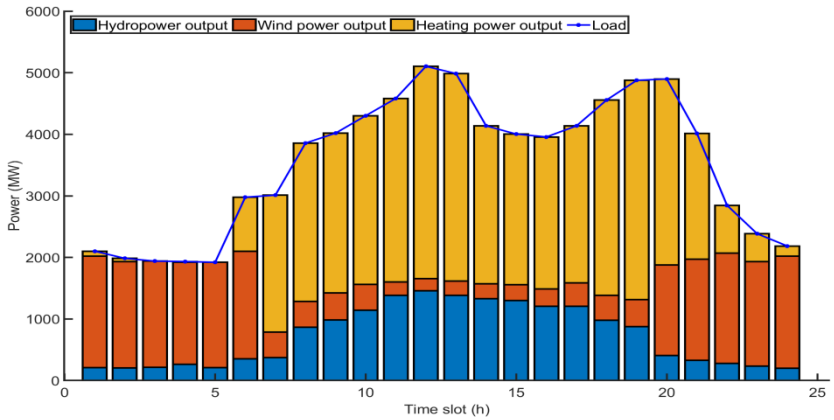

Figure 2: The generation output and the load profile of the units

As can be observed from Figure 2, during the peak hours of 11:00-13:00 and 18:00-20:00, the load is at its peak, and there is no flexibility peak shaving from the load side. Only the coordinated operation of source and load is implemented. During these peak electricity consumption hours, heating power units

ISSN 2522-3488 Vol. 8, Issue 4: 30-42, DOI: 10.25236/IJNDES.2024.080405

generate the most power, wind power generation is relatively low, and hydropower generation is at its peak level for the day. In other time, wind power generation dominates, with thermal and hydropower as auxiliary sources. However, due to the equivocal output power of renewable resources, thermal power units cannot be completely shut down, leading to the increased costs and a reduced proportion of renewable energy generation.

(2) Analysis of Scenario 2

Compared with Scenario 1, Scenario 2 incorporates the energy storage side for collaboration, specifically the collaboration between source-storage sides to provide electricity for the load side. In this scenario, the load side still does not engage in peak load shifting. The output power generation from the source-side units, the cycling of the energy storage system between charge and discharge states, and the load curve are shown in Figure 3.

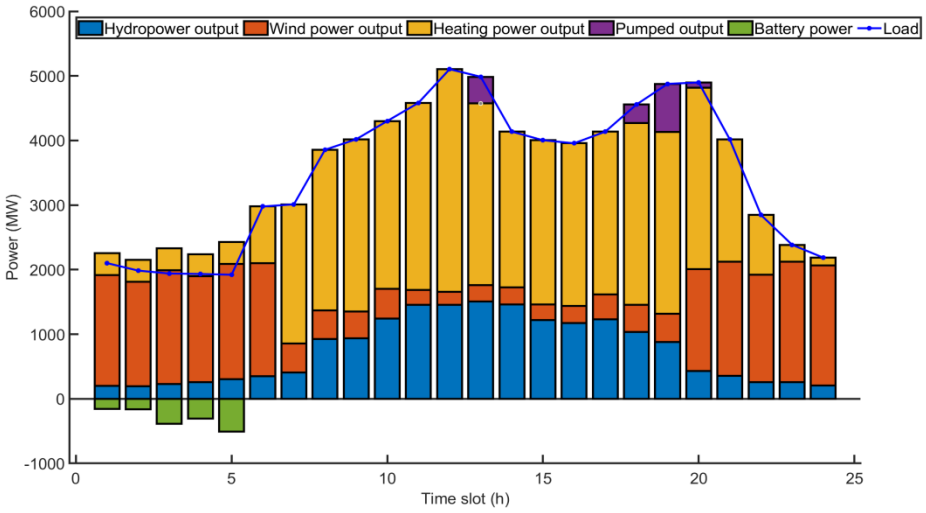

Figure 3: Generation Output and Load Curve Diagram

As illustrated in Figure 3, the time from 00:00 to 05:00 is the off-peak period of electric power utilization during the day. Due to the addition of the power storage facility for collaborative operation, the thermal power output can be appropriately increased during this period to provide energy for the pumped-storage hydroelectric facility to charge the batteries and store energy. Starting from 08:00, wind power output decreases while hydropower output increases, with thermal power generation remaining the primary source of power. However, since the pumped storage power station has stored energy in previous periods, the battery output reduces the percentage of power generated from heating during the peak electricity demand hours from 13:00 to 20:00. The incorporation of the energy storage system in this scenario leads to a reduction in the proportion of heating power generation during peak residential electricity consumption, an increase in the proportion of renewable power production, and a reduction in system operating costs due to the reduced thermal power output, resulting in higher renewable energy consumption.

The state of charge (SOC) of the battery in Scenario 2 is shown in Figure 4.

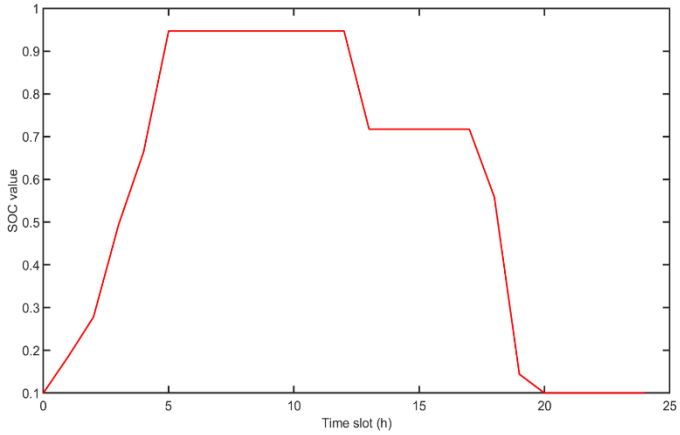

Figure 4: Battery State of Charge (SOC) Status Diagram

ISSN 2522-3488 Vol. 8, Issue 4: 30-42, DOI: 10.25236/IJNDES.2024.080405

As shown in Figure 4, the maximum and minimum limits of the battery charge are 10% and 95%. From 00:00 to 05:00, the battery is in a charging state. It remains idle from 05:00 to 12:00. The battery supplies power during the periods of 12:00-13:00 and 17:00-20:00, which corresponds to the battery output shown in Figure 3.

(3) Analysis of Scenario 3

Scenario 3 expands on Scenario 2 by additionally integrating the load side's demand response. This means that in Scenario 3, the system takes into account how the load side reacts to demand changes, which was not as emphasized in Scenario 2, allowing for load shifting and peak shaving based on the flexibility of the load side. This scheme implements coordinated operation between the source, storage, and load.

The effectiveness and feasibility of this scheme are analyzed from two perspectives: before and after optimization.

1) Comparison of Flexible Electric Load Distribution Prior to and following optimization

The flexible electric load distribution on the user side before and after optimization is shown in Figures 5 and 6, respectively.

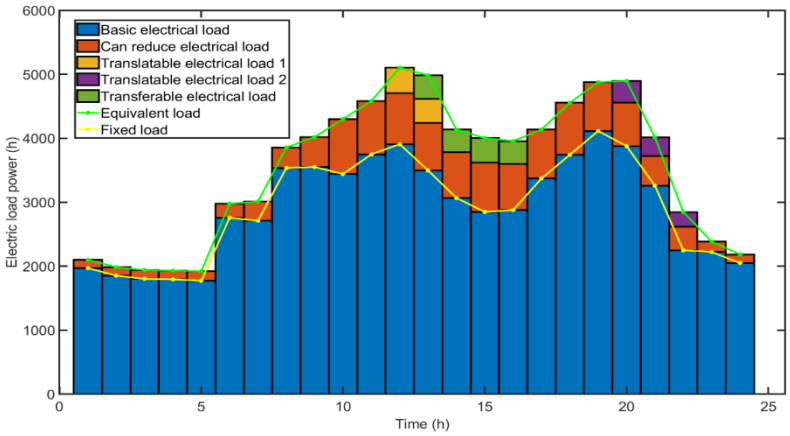

Figure 5: Pre-Optimization Distribution of Flexible Electric Loads on the User Side

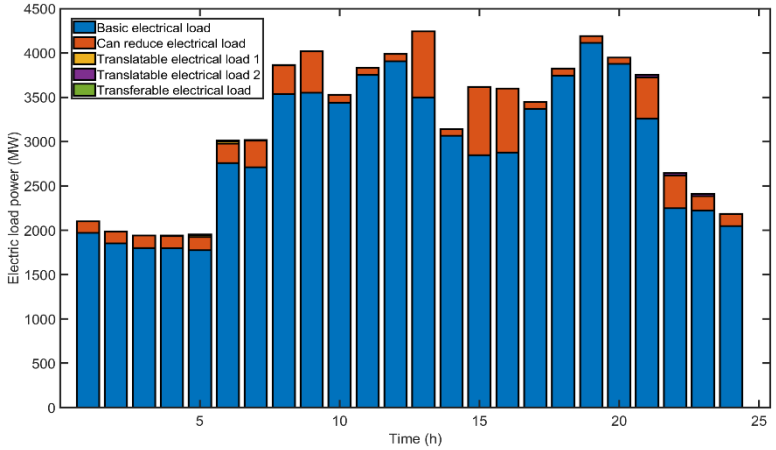

Figure 6: Post-Optimization Distribution of Flexible Electric Loads on the User Side

As Figures 5 and 6 illustrate, the system load before optimization contains a significant portion of shiftable and reducible loads, with a relatively high peak load around 5000MW. However, after optimization, the shiftable and reducible loads are reduced, and the load side undergoes peak load shifting, reducing the load in high-demand intervals and filling in the valleys, resulting in a smoother overall curve.

2) Comparison of Demand Response before and After Optimization

Due to the flexibility of the load side's demand response, the load is subject to peak shaving and valley filling, resulting in different degrees of smoothness in the load profile before and after enhancement measures. The comparison of demand response before and after optimization is shown in Figure 7.

ISSN 2522-3488 Vol. 8, Issue 4: 30-42, DOI: 10.25236/IJNDES.2024.080405

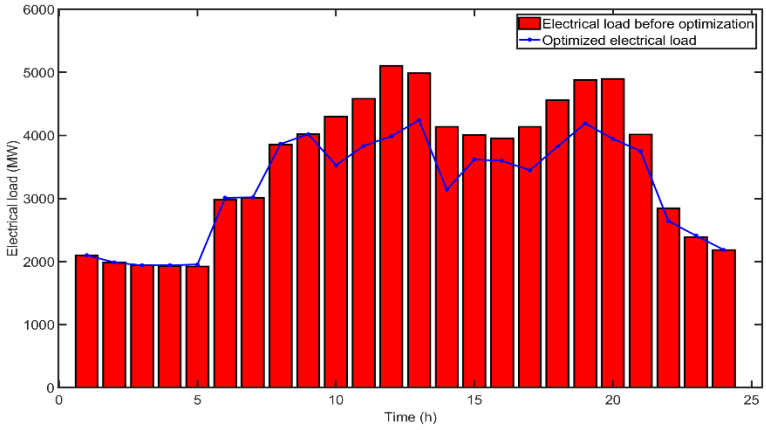

Figure 7: Demand Response Chart Before and After Optimization

In Figure 7, the optimized electric load curve is significantly smoother than the unoptimized curve, indicating that the load side's peak shaving and valley filling effectively adjust the high-power consumption during peak hours, making the system's supply-demand balance more stable and mitigating the issue of sudden changes in output from the source and storage sides caused by rapid increases and decreases in power usage.The optimized electric load balancing curve is shown in Figure 8.

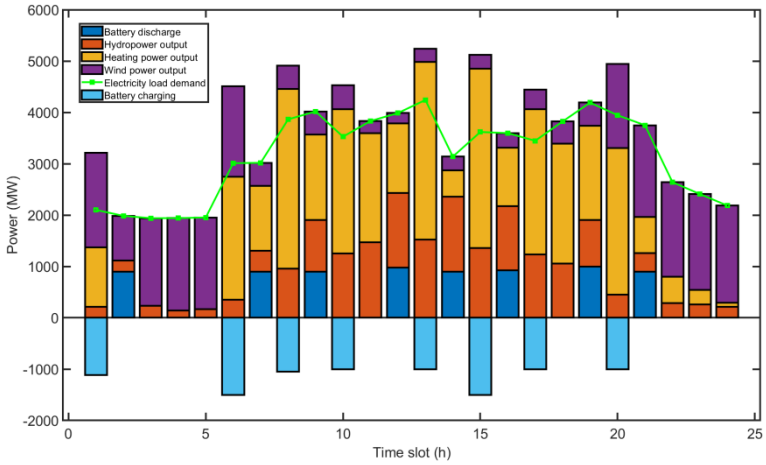

Figure 8: Electricity Load Balancing Chart

In Figure 8, the electric load demand curve becomes relatively stable, and the output of various units during peak hours is also relatively balanced. The charging of pumped storage units is more often powered by wind energy, and the battery also alleviates the output of thermal power during peak hours. Overall, the share of renewable energy sources is augmented, the system operating cost is lower, and it is more environmentally friendly.

4.3 Comprehensive analysis

The scheduling results of each scheme are presented in Table 4.

Table 4: Scheduling Results of Various System Schemes

	Total cost/ $	**Thermal power output (MW·h)**	**New energy proportion**
Scenario1	2,177,610.81	1,840.53	48.6%
Scenario2	2,121,623.68	1,845.88	47.7%
Scenario3	1,533,258.11	1,513.12	51.9%

As shown in Table 1, Contrasted with Scenarios 1 and 2, Scenario 3 neglects both the flexibility inherent in demand response and the coordinated functionality of the storage side, consequently leading to the most elevated operational expense. Compared to Scenario 2, Scenario 3 utilizes the flexibility of demand response to reduce and shift loads on the load side, effectively performing peak shaving and valley filling, which reduces the total system operating cost, refrain from thermal power generation, elevate the share of renewable energy sources, and enhance the utilization of renewable energy. In

ISSN 2522-3488 Vol. 8, Issue 4: 30-42, DOI: 10.25236/IJNDES.2024.080405

comparison to Scenario 1, Scenario 3 features an integrated operation with the storage component, along with the execution of load minimization and relocation strategies. This results in a heightened percentage of renewable energy integration and a diminution of the cumulative system operation costs. Hence, taking into account the harmonized operation among generation-storage-load components, coupled with load reduction and shifting measures, serves to escalate the share of renewable energy. This underscores the efficacy of Scenario 3 in driving a green transition whilst maintaining fiscal prudence, showcasing its superiority in both ecological and economic dimensions.

5. Conclusion

To optimize the scheduling of source-load-storage in the energy grid, the proportion of traditional thermal power generation is reduced, the consumption of renewable energy is enhanced, and lower the system operating cost. This research presents an optimization framework for the ideal structuring of a power system, encompassing aspects of generation, load, and storage. By engaging in comprehensive modeling and empirical case dissection, the ensuing deductions can be elucidated:

1) In accordance with the analysis of the output power balance and operation constraints of the supply side, storage side, and load side, it is feasible to achieve Collaborative operation between the source and storage to increase the proportion of renewable energy. The demand response of the load side can target specifically perform peak load shifting operation, providing the method for power system scheduling optimization.

2) Compared with traditional Scenario, according to hierarchical scheduling and load-side peak load shifting operation in load-side, the proposed strategy in this paper can better reduce operation cost and renewable energy curtailment of the system.

During the course of optimization, the output power and load change continuously over-time, which reflects the uncertainty of load-side power consumption in real situations scenarios and improves the flexibility of power supply on the supply side.

References

[1] A. K. Onaolapo, R. P. Carpanen, D. G. Dorrell and E. E. Ojo, "Assessment of Sustainable Development: a Nexus between Reliability, Greenhouse Gas Emissions and Renewable Energy Technologies," 2022 30th Southern African Universities Power Engineering Conference (SAUPEC), Durban, South Africa, 2022, pp. 1-5.

[2] A. Sarhan, V. K. Ramachandaramurthy, T. C. Sin, S. L. Walker, B. Salman and S. Padmanaban, "Assessment of Spatial and Temporal Modeling on Greenhouse Gas Emissions From Electricity Generation," in IEEE Access, vol. 11, pp. 97478-97492, 2023.

[3] D. -W. Kim, K. -H. Lee, J. -G. Kim, D. -S. Shin, T. -J. Ha and J. -W. Lee, "A Study on a Multi-Input/Output Power Supply System that can Improve Energy Operation Efficiency and Reduce Greenhouse Gas Emissions in small ship," 2021 24th International Conference on Electrical Machines and Systems (ICEMS), Gyeongju, Korea, Republic of, 2021, pp. 2476-2481.

[4] J. Shadiq, I. Rosyadi and Y. P. Adianto, "Could Economic Dispatch and Unit Commitment with Emission Constraints Reduce Power System Costs? A Case Study on Java-Madura-Bali Power System," 2023 4th International Conference on High Voltage Engineering and Power Systems (ICHVEPS), Denpasar Bali, Indonesia, 2023, pp. 788-792.

[5] Z. Qiang, D. Jia, W. Gu and C. Chen, "Full Topology Simulation Model and Control Strategy for Photovoltaic System and Energy Storage System under New Power System," 2023 IEEE/IAS Industrial and Commercial Power System Asia (I&CPS Asia), Chongqing, China, 2023, pp. 1727-1732.

[6] L. Yan, T. Xinshou, H. Jianzu and L. Chao, "Research on Reactive Power Planning Technology of Power Grid Containing UHVDC System with High Proportion of Renewable Energy Integration," 2020 IEEE International Conference on High Voltage Engineering and Application (ICHVE), Beijing, China, 2020, pp. 1-4.

[7] I. Zicmane, K. Berzina, T. Lomane and K. Kasperjuks, "Improving the Energy Efficiency of an Autonomous Power System with Renewable Sources," 2018 International Conference on Intelligent and Innovative Computing Applications (ICONIC), Mon Tresor, Mauritius, 2018, pp. 1-6.

[8] D. Braga, "Integration of Energy Storage Systems into the Power System for Energy Transition towards 100% Renewable Energy Sources," 2021 10th International Conference on ENERGY and ENVIRONMENT (CIEM), Bucharest, Romania, 2021, pp. 1-5.

ISSN 2522-3488 Vol. 8, Issue 4: 30-42, DOI: 10.25236/IJNDES.2024.080405

[9] X. Meng et al., "Bi-Level Joint Planning of Transmission Network and Energy Storage System to Enhance Flexibility," 2023 International Conference on Power Energy Systems and Applications (ICoPESA), Nanjing, China, 2023, pp. 364-368.
[10] Y. Zhang, K. Cui, Y. Guo and Y. Ding, "An Optimal Dispatching Model of Active Distribution Network Based on the Collaboration of Source-Load-Storage," 2023 3rd International Conference on New Energy and Power Engineering (ICNEPE), Huzhou, China, 2023, pp. 1061-1068.
[11] X. Liu, H. Wang, G. Yu, B. Wang, Y. Sun and X. Guan, "A Power Grid Capacity Margin Model and Calculation Method Considering the Interaction of Source-Load-Storage," 2023 IEEE/IAS Industrial and Commercial Power System Asia (I&CPS Asia), Chongqing, China, 2023, pp. 2226-2232.
[12] Y. Li, H. Liu, Y. Chi, X. Fan, X. Tian and Z. Zhang, "Requirement Analysis on Large-scale Renewable Energy DC Collection and Transmission Technology," 2020 4th International Conference on HVDC (HVDC), Xi'an, China, 2020, pp. 410-414.
[13] S. Paul, T. Dey, P. Saha, S. Dey and R. Sen, "Review on the development scenario of renewable energy in different country," 2021 Innovations in Energy Management and Renewable Resources(52042), Kolkata, India, 2021, pp. 1-2.